Study on a Vibration Reduction System for Lift Roller Guides

Yosuke Shima[1] and Osamu Furuya[2]

[1]Graduate School of Tokyo Denki University, Ishizaka, Hatoyama-cho, Hiki-gun, Saitama 350-0394 Japan
[2]Division of Mechanical Engineering, School of Science and Engineering, Tokyo Denki University, Ishizaka, Hatoyama-cho, Hiki-gun, Saitama 350-0394 Japan

Abstract. Lift roller guides require time and effort for maintenance and replacement, so if they can be extended in life, advantages such as reduced maintenance frequency, cost reduction, and improved reliability can be obtained. In this research, authors propose roller guides that achieve long life by changing the material of the roller and have both ride comfort and durability. To decrease the vibration of lift cabin, an analytical model for calculating the time history response of the lift cabin will be constructed, and the vibration control effect will be verified by simulation incorporating spring and damping elements based on the experimental results. Through analytical and experimental approach, a design way for a roller guide that has optimal riding comfort and durability within the range of safety regulations is proposed.

1   INTRODUCTION

In recent years, the number of lifts has been increasing, as facility investment for the new construction of high-rise buildings by redevelopment in urban areas, barrier-free and renewal of old age has become active. Demand for lifts is expected to increase further in the future due to the impact of emerging countries and redevelopment. Roller guides form a part of the car-frame guiding system, the elastic- damping properties of the roller guide shoe (wheel tire), and if included, of additional spring-damper elements provide passive vibration control mechanism installed between the rail in the lift shaft and the cabin on which the person rides, and plays the role of smoothly moving up and down while suppressing vibration. However, with the spread of lifts, there is a shortage of human resources responsible for maintenance. In particular, since roller guides require maintenance and replacement, it is considered meaningful to extend their service life (durability) to reduce maintenance frequency, cost, and reliability. If the rollers are hardened to increase durability, the problem occurs that comfortability and noise will deteriorate. In this study, the problem of vibration and abrasion in the roller guides is focused, and aimed to examine the specification conditions of the roller guides to achieve both comfortability and durability. Specifically, some experiments to investigate the mechanical properties and durability of the roller guides are conducted.

2   ROLLER GUIDES

Much of the vibration in the moving cabin of the lift is attributed to the distortion of the guide rail installed in the lift shaft. Figure 1 shows the structure of lift cabin. The main cause of distortion is low accuracy during installation [1], or distortion due to age [2], and existing lifts require drastic renovation for improvement. The distortion of the guide rail propagates inside the cabin along the roller guides, the frame and the rubber mounts. Figure 2 shows the actual roller guides used for the experimental and analytical investigations.

The roller guides handled here are composed of a coil spring, a control arm and a circular roller. The material of the roller part is natural rubber, but it cracks due to wear and eventually peels off. As a countermeasure, it is common to thoroughly implement preventive replacement to increase hardness and durability.

In this research, vibration and durability problems in the roller guides are focused on, and after replacing the material of the roller part to secure the durability, the specification conditions of the roller guide that is compatible with the riding comfort is aimed to examine. Through the analytical and experimental process, the roller guide that achieves both optimum riding comfort and durability within the range that meets safety regulations is designed. Active roller guides are effective in suppressing vibration significantly, and manufacturers are working on development, but there are problems such as high cost and difficulty in adjustment [3].

In this study, the roller guide system that prioritizes compatibility and improves existing passive roller guides to reduce vibration levels at low cost is developed. In the research, the vibration level at which passengers do not feel uncomfortable sets to rms Acc. 0.1 m/s^2 [4] and sets a displacement as small as possible that does not make contact with other structures as an allowable limit. The roller guides used in this study have a low flatness as shown in Fig. 2. Since a change in mechanical characteristics due to displacement is expected, loading test using a hydraulic servo actuator is conducted. Furthermore, the roller made by urethane elastomer with hardness of JIS-A standard 95 degrees, which has excellent wear resistance, is prototyped and the same experiment is performed. This material is also used in roller guides for railroad track of public transportation system and play facilities, such as Automated Guideway Transit, roller coaster and so on.

Figure 1 Structure of lift cabin
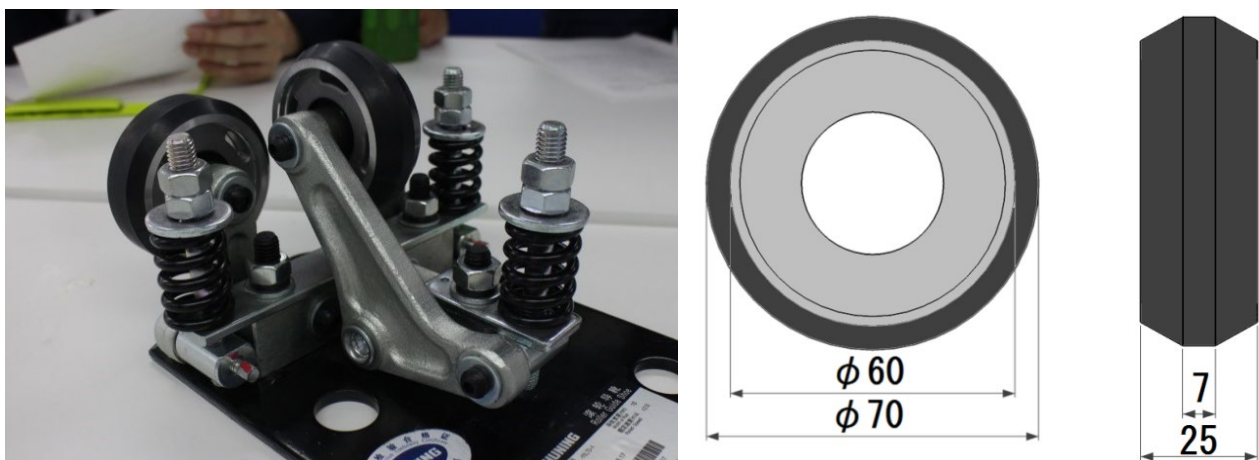
Figure 2 Roller Guides

3   ANALYSIS OF LIFT CAR VIBRATION

3.1   Analytical Model

In order to calculate the lateral vibration of the running lift, an analytical model [5] that imitates an actual 6 person ride machine was constructed. In this model, the vibration transmitted from the rail roughness to the cabin via the roller guide, the coil spring, the frame, and the rubber mounts [6] are calculated. An eight-degree-of-freedom analytical model was constructed to calculate the horizontal movement of the four rollers and the horizontal movement and rotation of the frame and cabin. The centre of rotation is same for the frame and the cabin. Waves of the same waveform are input to the upper and lower rollers with a time difference. Acceleration/deceleration of the lift was not included. Figure 3 shows the 8-DOF analytical model. MATLAB2020a was used for the analysis. Figure 4 shows the overview of model.
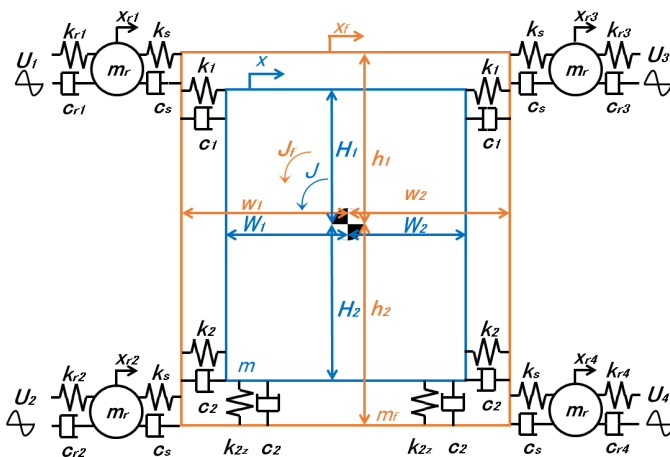
Figure 3 Analytical model   **Figure 4 Overview of model**
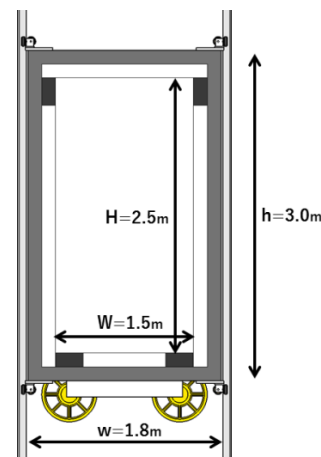
Eq.1 to 8 shows the Equation of Motion (EOM) in this model. In here,

U_n: input displacement,

k_{rn}: stiffness of roller, c_{rn}: damping coefficient of roller, m_r: mass of roller, x_{rn}: displacement of roller,

"n" represents each number from 1 to 4.

k_s: stiffness of coil spring, c_s: damping coefficient attaching to coil spring,

k_1: stiffness of upper rubber mount, c_1: damping coefficient of upper rubber mount,

k_2: stiffness of lower rubber mount, c_2: damping coefficient of lower rubber mount,

m: mass of frame, x_f: displacement of frame, θ_f: rotation of frame, J_f: Moment of inertia in frame,

w_1: width of frame, w_2: width of frame, h_1: height of frame, h_2: height of frame,

M: mass of cabin, x: displacement of cabin, θ: rotation of cabin, J: Moment of inertia in cabin,

W_1: width of cabin, W_2: width of cabin, H_1: height of cabin, H_2: height of cabin

In the actual response analysis, the following variables are substituted for the above variables.

m = 1200 kg, w_1 =0.9 m, w_2 = 0.9 m, h_1 = 1.5 m, h_2 = 1.5 m,

M =1000 kg, W_1 =0.75 m, W_2 = 0.75 m, H_1 = 1.25 m, H_2 =1.25 m

k_1 = 400 N/mm, k_2 = 400 N/mm ,k_{2z} = 2000 N/mm , c_1 = 400 N·s/mm , c_2 = 400 N·s/mm

$$m_r \ddot{x}_{r1} = -k_{r1}\left(x_{r1} - U_{r1}\right) - c_{r1}\left(\dot{x}_{r1} - \dot{U}_{r1}\right) - k_s\left(x_{r1} - \left(x_f - h_1\theta_f\right)\right) - c_s\left(\dot{x}_{r1} - \left(\dot{x}_f - h_1\dot{\theta}_f\right)\right) \tag{1}$$

$$m_r \ddot{x}_{r2} = -k_{r2}\left(x_{r2} - U_{r2}\right) - c_{r2}\left(\dot{x}_{r2} - \dot{U}_{r2}\right) - k_s\left(x_{r2} - \left(x_f + h_2\theta_f\right)\right) - c_s\left(\dot{x}_{r2} - \left(\dot{x}_f + h_2\dot{\theta}_f\right)\right) \tag{2}$$

$$m_r \ddot{x}_{r3} = -k_{r3}\left(x_{r3} - U_{r3}\right) - c_{r3}\left(\dot{x}_{r3} - \dot{U}_{r3}\right) - k_s\left(x_{r3} - \left(x_f - h_1\theta_f\right)\right) - c_s\left(\dot{x}_{r3} - \left(\dot{x}_f - h_1\dot{\theta}_f\right)\right) \tag{3}$$

$$m_r \ddot{x}_{r4} = -k_{r4}\left(x_{r4} - U_{r4}\right) - c_{r4}\left(\dot{x}_{r4} - \dot{U}_{r4}\right) - k_s\left(x_{r4} - \left(x_f + h_2\theta_f\right)\right) - c_s\left(\dot{x}_{r4} - \left(\dot{x}_f + h_2\dot{\theta}_f\right)\right) \tag{4}$$

$$\begin{aligned}
mx_f =\ &-k_s\left(4x_f - x_{r1} - x_{r2} - x_{r3} - x_{r4}\right) - c_s\left(4x_f - \dot{x}_{r1} - \dot{x}_{r2} - \dot{x}_{r3} - \dot{x}_{r4}\right) \\
&+2k_s\left(h_1 - h_2\right)\theta_f + 2c_s\left(h_1 - h_2\right)\dot{\theta}_f \\
&-2\left(k_1 + k_2\right)\left(x_f - x\right) - 2\left(c_1 + c_2\right)\left(\dot{x}_f - \dot{x}\right) \\
&+2\left(k_1 H_1 - k_2 H_2\right)\left(\theta_f - \theta\right) + 2\left(c_1 H_1 - c_2 H_2\right)\left(\dot{\theta}_f - \dot{\theta}\right)
\end{aligned} \tag{5}$$

$$\begin{aligned}
J_f \ddot{\theta}_f =\ &k_s h_1\left(2x_f - x_{r1} - x_{r3}\right) - k_s h_2\left(2x_f - x_{r2} - x_{r4}\right) \\
&+c_s h_1\left(2\dot{x}_f - \dot{x}_{r1} - \dot{x}_{r3}\right) - c_s h_2\left(2\dot{x}_f - \dot{x}_{r2} - \dot{x}_{r4}\right) \\
&-2k_s\left(h_1^2 + h_2^2\right)\theta_f - 2c_s\left(h_1^2 + h_2^2\right)\dot{\theta}_f \\
&+2\left(k_1 H_1 - k_2 H_2\right)\left(x_f - x\right) + 2\left(c_1 H_1 - c_2 H_2\right)\left(\dot{x}_f - \dot{x}\right) \\
&-2\left(k_1 H_1^2 + k_2 H_2^2\right)\left(\theta_f - \theta\right) - 2\left(c_1 H_1^2 + c_2 H_2^2\right)\left(\dot{\theta}_f - \dot{\theta}\right) \\
&-k_2\left(W_1^2 + W_2^2\right)\left(\theta_f - \theta\right) - c_2\left(W_1^2 + W_2^2\right)\left(\dot{\theta}_f - \dot{\theta}\right)
\end{aligned} \tag{6}$$

$$\begin{aligned}
M\ddot{x} =\ &-2\left(k_1 + k_2\right)\left(x - x_f\right) - 2\left(c_1 + c_2\right)\left(\dot{x} - \dot{x}_f\right) \\
&+2\left(k_1 H_1 - k_2 H_2\right)\left(\theta - \theta_f\right) + 2\left(c_1 H_1 - c_2 H_2\right)\left(\dot{\theta} - \dot{\theta}_f\right)
\end{aligned} \tag{7}$$

$$\begin{aligned}
J\ddot{\theta} =\ &2\left(k_1 H_1 - k_2 H_2\right)\left(x - x_f\right) + 2\left(c_1 H_1 - c_2 H_2\right)\left(\dot{x} - \dot{x}_f\right) \\
&-2\left(k_1 H_1^2 + k_2 H_2^2\right)\left(\theta - \theta_f\right) - 2\left(c_1 H_1^2 + c_2 H_2^2\right)\left(\dot{\theta} - \dot{\theta}_f\right) \\
&-k_2\left(W_1^2 + W_2^2\right)\left(\theta - \theta_f\right) - c_2\left(W_1^2 + W_2^2\right)\left(\dot{\theta} - \dot{\theta}_f\right)
\end{aligned} \tag{8}$$

3.2   Modeling on mechanical characteristics for the roller guides

The response displacement of the commonly used rubber roller (hereinafter called "rubber roller") and the prototyped urethane roller (hereinafter called "urethane roller") with increased hardness, the stiffness and the damping coefficient dependence on the vibration frequency and displacement, are investigated. In these experiments, mechanical characteristics for the roller guides in a loading experiment [7,8] using a hydraulic servo actuator is investigated, and an operation test using a miniature test apparatus is evaluated. Figures 5 and 6 shows the experimental results. The hardness

and damping coefficient of the urethane roller are about 3 times that of the rubber roller. In addition, the amplitude dependence, which is a characteristic of urethane elastomer with hardness of JIS-A standard 95 degrees, was confirmed.

The dependency functions for mechanical characteristic of roller guide in amplitude-dependency and frequency-dependency are obtained from the experimental results. Eq.9 to 12 shows the mechanical characteristics for the roller guides. These formulas are derived from the amplitude dependency and frequency dependency obtained from the loading test of the roller guide. Therefore, in this formula, if the arbitrary frequency and amplitude are substituted as variables, the stiffness and damping coefficient under arbitrary condition are calculated.
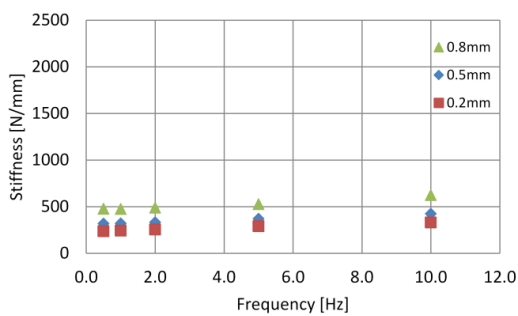
(a)Frequency dependency on
stiffness in rubber roller
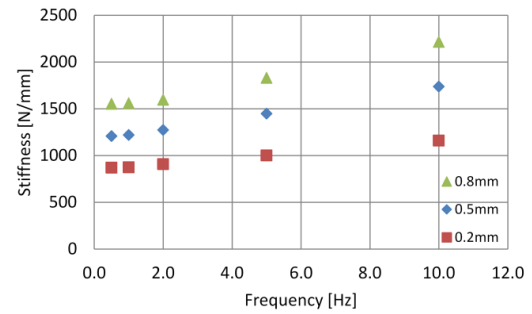
(c)Frequency dependency on
stiffness in urethane roller
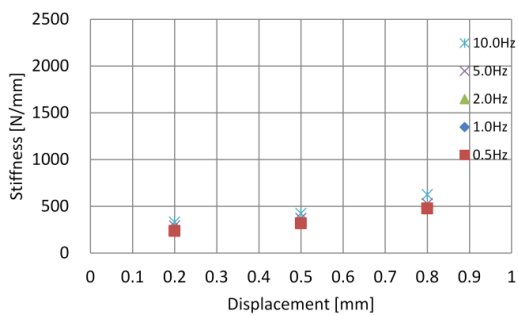
(b)Displacement dependency on
stiffness in rubber roller
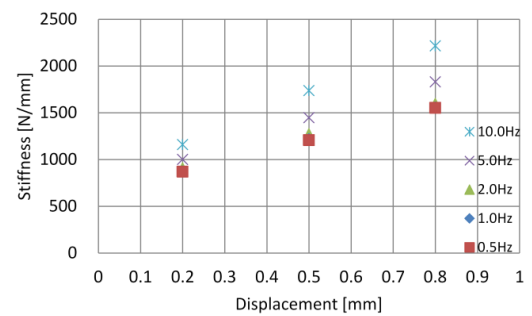
(d)Displacement dependency on
stiffness in urethane roller

Figure 5 Comparison between stiffness of rubber roller and urethane roller
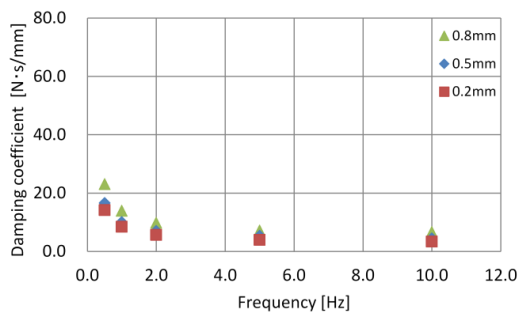
(e)Frequency dependency on
damping coefficient in rubber roller
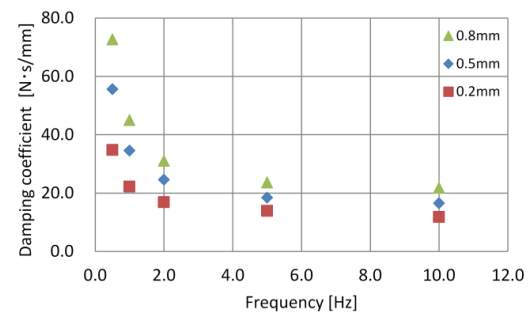
(g)Frequency dependency on
damping coefficient in urethane roller
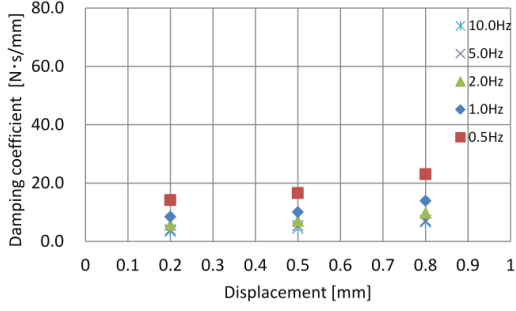
(f)Displacement dependency on
damping coefficient in rubber roller
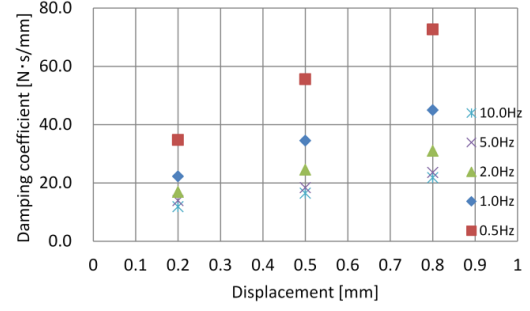
(h)Displacement dependency on
damping coefficient in urethane roller

Figure 6 Comparison between damping coefficient of rubber roller and urethane roller

In here, x_i: displacement of input wave [mm], f_i: vibration frequency [Hz]

Rubber roller

$$k_r = (9.76 f_i + 377) x_i + 7.43 f_i + 148 [\text{N} / \text{mm}] \tag{9}$$

$$c_r = 9.96 f_i^{-0.337} x_i + 6.54 f_i^{-0.525} [\text{N} \cdot \text{s/mm}] \tag{10}$$

Urethane roller

$$k_r = (68.1 f_i + 1060) x_i + 19.2 f_i + 637 [\text{N} / \text{mm}] \tag{11}$$

$$c_r = 39.2 f_i^{-0.465} x_i + 16.2 f_i^{-0.277} [\text{N} \cdot \text{s/mm}] \tag{12}$$

3.3   Analytical Result

The vibration reduction effect of the lift cabin is verified using the analytical model introduced in 3.1. Although the running speed set to be arbitrarily in the analytical model, this time it was set to 105m/min as a medium speed. The running speed affects rail bends and interval of gap. Figure 7 shows the input waveform. It is difficult to measure the actual roughness of the rail. Instead of this, the artificial synthetic wave was used to simulate various irregularities of roughness on the rail. Since the main component of the waveform is 5Hz on the left side figure and 2Hz on the right side figure, the parameter f_i that affects the stiffness and damping of the roller is adjusted to these dominant frequencies. The parameter x_i changes moment by moment according to the displacement of input. The max displacement of rail roughness is 0.1mm. The wave inputs to the upper, lower, left and right rollers. Furthermore, a sinusoidal wave simulating a maximum rail distortion of 3 mm was synthesized on one side, and the 0.5mm gap was synthesized on both sides. Acceleration on the cabin floor: $\ddot{x} + H_2 \cdot \ddot{\theta}$, Displacement: x, and Rotation: θ of the cabin part are obtained by response analysis.

Figure 8 shows the vibration waveform when a rubber roller and a urethane roller are installed. The installation of urethane guide rollers improves the strength more than rubber rollers, but the riding comfort may deteriorate, so it is necessary to consider the concept of damping of the entire system. The periodic fluctuations of displacement and rotation are the effects of rail distortion. In the next step, a coil spring is installed between the roller and the cabin to reduce response vibration. Figures 9 and 10 shows the verification of the optimum mechanical characteristics and the vibration waveform at that time. The maximum response of the coil spring stiffness was set to be smaller than

the roller stiffness. Under the condition, the stiffness that satisfies the rms Acc. of 0.1 m/s^2 is in the range of 800 N/mm. It was attempted to reduce vibration by substantially adding damping to the coil spring. As a result, reduction of rms Acc. was confirmed with a damping ratio of 7.5%. Table 1 compares rms Acc. and Max Acc. under each condition. The rms Acc. when using the rubber roller was set to 100% and expressed as the vibration reduction level. As a result, the rms Acc. was reduced by up to 60% by adding the coil spring under the analysis conditions of this time.
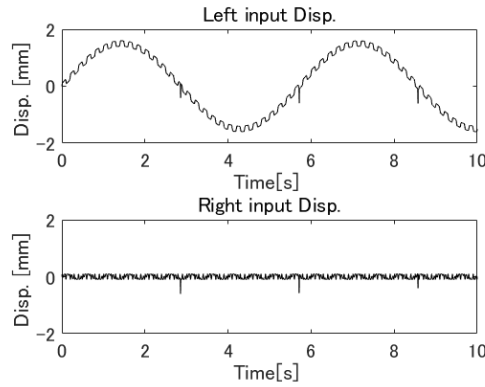
Figure 7 Input waveform
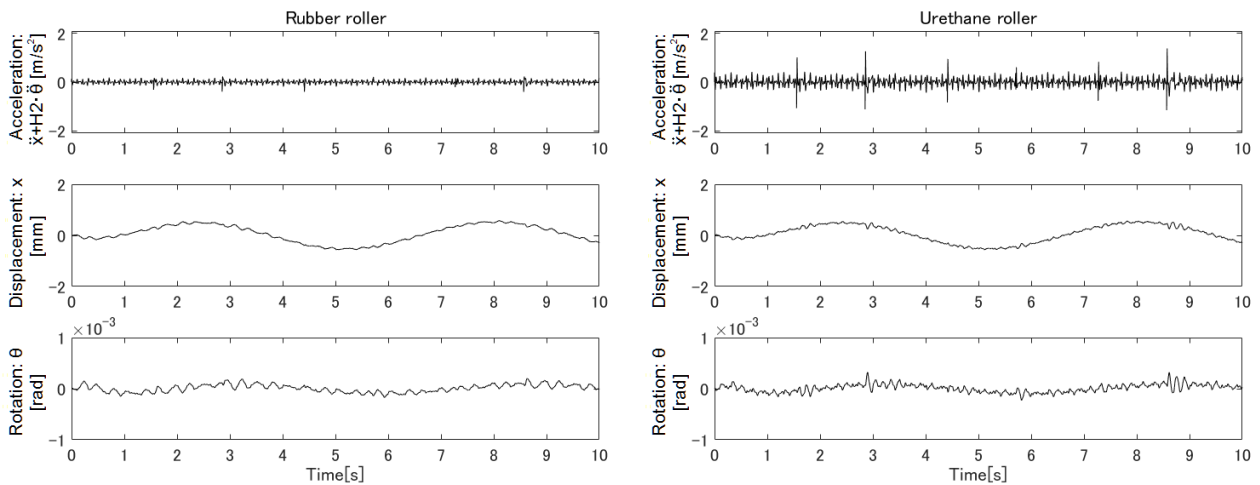
Figure 8 Comparison between rubber roller and urethane roller
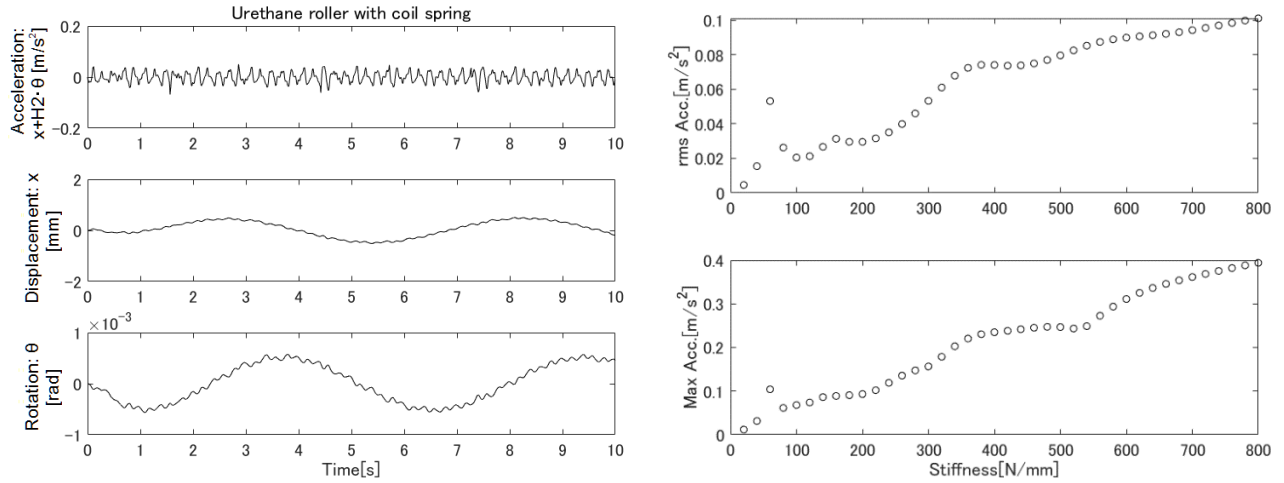
Figure 9 State of optimizing stiffness of coil Spring
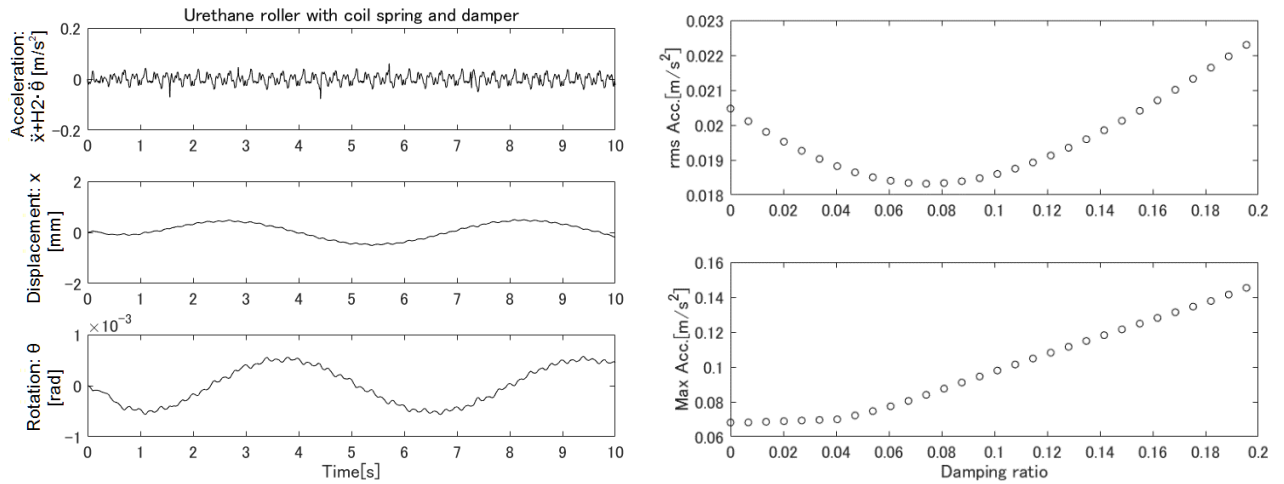
Figure 10 State of optimizing stiffness of damper

Table 1 Response of lift cabin in each situation

	Rubber roller	Urethane roller	Urethane roller with coil spring	Urethane roller with coil spring and damper
Max Acc. [m/s²]	0.400	1.26	0.0682	0.0840
rms Acc. [m/s²]	0.0645	0.150	0.0205	0.0183
Vibration level [%]	100	233	31.8	28.4

4   DRIVING EXPERIMENT USING THE MINIATURE TEST SYSTEM FOR ROLLER GUIDES

The experiment using the actual lift is expensive and time-consuming, and it is not realistic to repeat the durability test. In this study, the reduction tester for roller guides was made, and conducted a running test. The experiment equipment consists of a disk that imitates the rail roughness and an iron plate that imitates the cabin. The size of this equipment is 1129 x 930 x 710 mm. By attaching a roller guide to a disk and running it, the horizontal vibration of the cabin and the durability of the roller are verified. Figure 12 shows the overview of the experiment equipment. Shim tape with a width of 10 mm is attached to the disk, and by running in this state, the vibration transmission when overcoming the projection is simulated. The thickness of one shim tape is 0.1mm, and any number of these can be stacked. The cabin can rotate freely in the horizontal and rotational directions by means of linear guides and bearings. An accelerometer (KYOWA AS2GB accelerometer and TEAC es8 data recorder) was attached to the centre of the cabin, and recording was performed at a sampling frequency of 1000Hz. The analytical model is a combination of the frame and cabin of the model introduced in 3.1. Equations (1) to (4) are the same as the model introduced in 3.1, but the equation of the mass part is different. Figure 11 shows the 6-DOF analytical model. Equation (13), (14) shows the equation of motion in mass part.
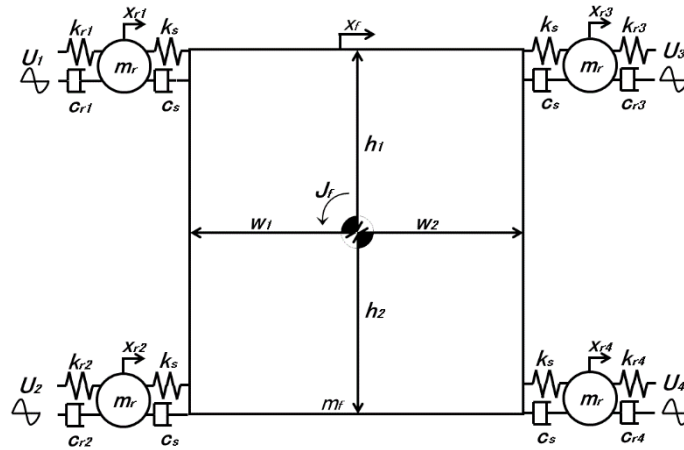
Figure 11 6-DOF analytical model

$$mx_f = -k_s \left(4x_f - x_{r1} - x_{r2} - x_{r3} - x_{r4} \right) - c_s \left(4\dot{x}_f - \dot{x}_{r1} - \dot{x}_{r2} - \dot{x}_{r3} - \dot{x}_{r4} \right)$$
$$+ 2k_s \left(h_1 - h_2 \right) \theta_f + 2c_s \left(h_1 - h_2 \right) \dot{\theta}_f \tag{13}$$

$$J_f \ddot{\theta}_f = k_s h_1 \left(2x_f - x_{r1} - x_{r3} \right) - k_s h_2 \left(2x_f - x_{r2} - x_{r4} \right) + c_s h_1 \left(2\dot{x}_f - \dot{x}_{r1} - \dot{x}_{r3} \right) - c_s h_2 \left(2\dot{x}_f - \dot{x}_{r2} - \dot{x}_{r4} \right)$$
$$- 2k_s \left(h_1^2 + h_2^2 \right) \theta_f - 2c_s \left(h_1^2 + h_2^2 \right) \dot{\theta}_f \tag{14}$$

Parameter used in the model: m = 15 kg, w_1 =0.125 m, w_2 = 0.125 m, h_1 = 0.115 m, h_2 = 0.115 m

Figure 13 shows the input waveform and analysis and test results. The waveform that reproduced the protrusion was input to the analysis program for the actual machine and compared with the test results. When comparing the experiment results and the analysis results, the peak waveform periods are shifted. This is probably because the rotation of the disk is unstable due to insufficient torque of the induction motor on the equipment. Although there are other differences in acceleration levels that are thought to be due to the shim mounting method, the reproducibility is generally good, and it can be

used to develop elements such as rollers and springs. In the future, conducting a verification experiment to verify the optimum value calculated using the analysis model and conducting a durability test of roller guides made of different materials are considered.
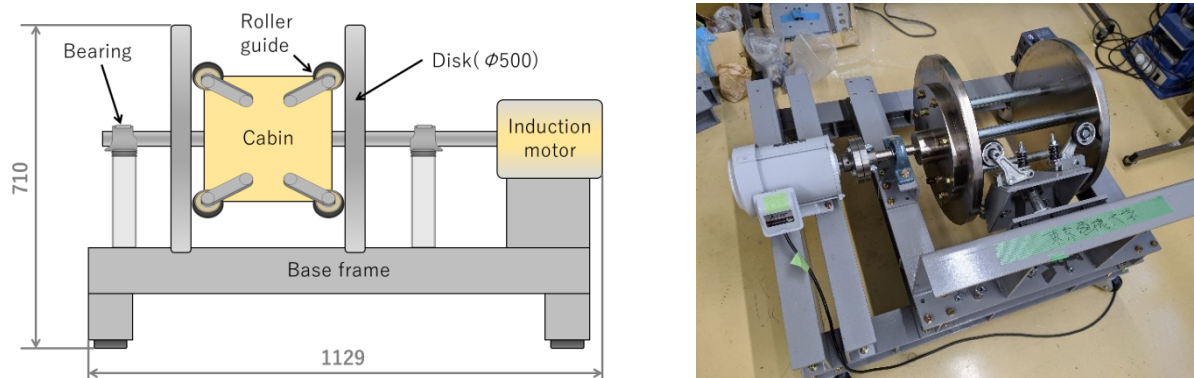
Figure 12 Overview of equipment
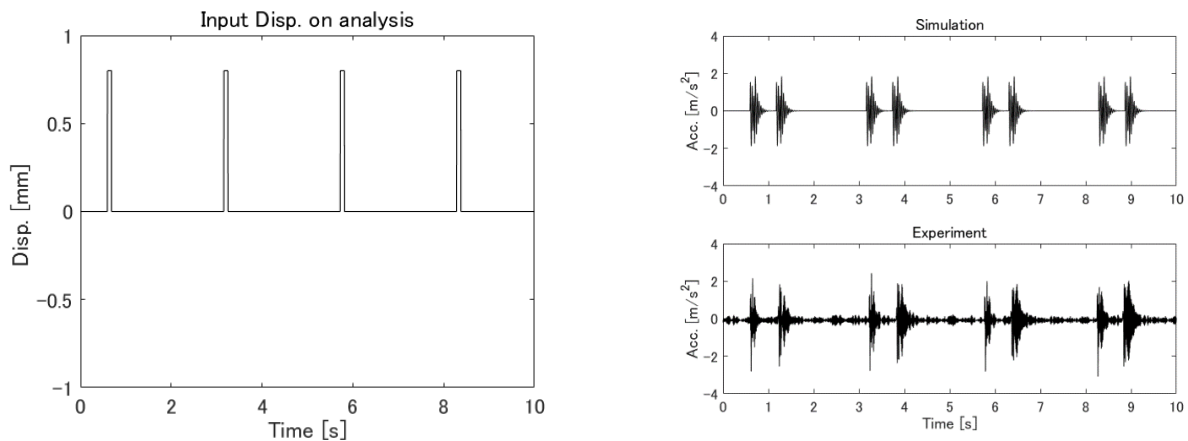
Figure 13 Experiment and Analysis result

5   CONCLUSION

In this study, in order to improve the durability of the roller guides and enhance the vibration reduction effect, a simulation analysis was performed using an 8-DOF analysis model. As a result, it was confirmed that the vibration can be sufficiently reduced to 87.7% at maximum by using the coil spring and the damping even if the roller hardened to enhance the durability is used. The Acc. at this time is much lower than 0.1m/s^2, and it is thought that a comfortable ride for passengers can be realized.

This time, the stiffness of the coil spring was calculated within the range of less than 800 N/mm. In general, the weight of the cabin is lighter and the response tends to be larger when the number of passengers is smaller than when the passengers are full. The rms Acc. is less than the standard 0.1 m/s^2 even when there is no load. The key point for vibration reduction when using a urethane roller with enhanced durability is the setting of coil spring. Also, by adding damping, it is possible to further suppress rms Acc. while maintaining the same Max Acc. In the actual lift, the stroke of the coil spring is limited because the frame does not come into contact with other structures. In consideration of the deviation of the riding position and the disturbance such as earthquake, the stiffness is set to be larger than the value that can suppress the vibration in the analysis to the greatest extent. In addition, the

waveform used in the simulation is a little worse than that expected in the actual machine, but it can satisfy the ride comfort sufficiently.

Also, a reduction test device for roller guides was manufactured for the durability test. Here, a rail roughness including protrusions was reproduced by placing shims on the surface of the device. Comparing the operation test results with the analytical model simulation results, the reproducibility is generally good despite some problems, and it is considered that it can be used for the element development of rollers and springs.

In the future, a durability experiment of the roller guide using a reduction tester and verifying the vibration reduction effect of the coil spring with damping will be performed. By installing the spring, it can be expected to greatly reduce both acceleration and displacement. Particularly effective in situations where the rail roughness is bad (rough) as verified by simulation. Also, the response in a driving process from start-up to stop will be investigated including increase/decrease of load/eccentricity.

REFERENCES

[1]   Satoshi Fujita, Hiroshi Kamaike, Motoo Shimoaki, and Keisuke Minagawa, "Elevator and Escalator Engineering", 156-160, (2019) (in Japanese)

[2]   Nobuyoshi Mutoh, Kenkichi Kagomiya, Toshiaki Kurosawa, Masahiro Konya, and Takeki Andoh, "Horizontal Vibration Suppression Method Suitable for Super-High-Speed Elevators", *Transactions on Electrical and Electronic Engineering*, Vol.118-D, No.3, (1998) (in Japanese)

[3]   Naoaki Noguchi, Atsushi Arakawa, Koichi Miyata, Takuya Yoshimura and Seiichi Shin, "Study on Active Vibration Control for High-Speed Elevators". *Journal of System Design and Dynamics*, Vol.5, No.1, 164-179 (2011).

[4]   Kiyoshi Funai, "Technologies of Safety and Ride Comfort for Elevators". *International Association of Traffic and Safety Sciences*, Vol.27, No.2, 31-39 (2002) (in Japanese)

[5]   Hiroyuki Kimura, Mimpei Morishita, Shigeo Nakagaki, "Simulation Techniques for Elevators", *TOSHIBA Review*, Vol.58, 42-45,(2003) (in Japanese)

[6]   Aritomo Nakano, "Types and properties of anti-vibration materials", *Journal of environmental conservation engineering*, Vol.20, No.6, 400-402, (1991) (in Japanese)

 [7]   Kazuhito Misaji, Hideki Kato, and Koichi Shibata, "Vibration Analysis of Rubber Vibration Isolators of Vehicle Using the Restoring Force Model of Power Function Type", *Transactions of the Japan society of mechanical engineers. C*, Vol.60, No.578, 679-685, (1994)

[8]   Satoshi Fujita, Osamu Furuya, Yoji Suizu, Yasuhiro Kasahara, Takayuki Teramoto, Haruyuki Kitamura, "Vibration Control of High-Rise Buildings using High-Damping Rubber Damper (2nd Report, Loading Tests and Design Formula for Cylinder-Type High-Damping Rubber Damper)", *Transactions of the Japan society of mechanical engineers. C*, Vol.61, No.585, 1885-1890, (1995) (in Japanese)

ACKNOWLEDGEMENT

BIOGRAPHICAL DETAILS

Yosuke Shima is master's course student in mechanical engineering of Tokyo Denki University. He researches vibration reduction of lift cabin.

Prof. Osamu Furuya is Professor in Tokyo Denki University. Recently main research object is research and development of vibration reduction for various structures and seismic safety for important facilities.